Article

Solution Structure of Vanabin2, a Vanadium(IV)-Binding Protein from the Vanadium-Rich Ascidian *Ascidia sydneiensis samea*

Toshiyuki Hamada, Miwako Asanuma, Tatsuya Ueki, Fumiaki Hayashi, Naohiro Kobayashi, Shigeyuki Yokoyama, Hitoshi Michibata, and Hiroshi Hirota

J. Am. Chem. Soc., **2005**, 127 (12), 4216-4222• DOI: 10.1021/ja042687j • Publication Date (Web): 02 March 2005

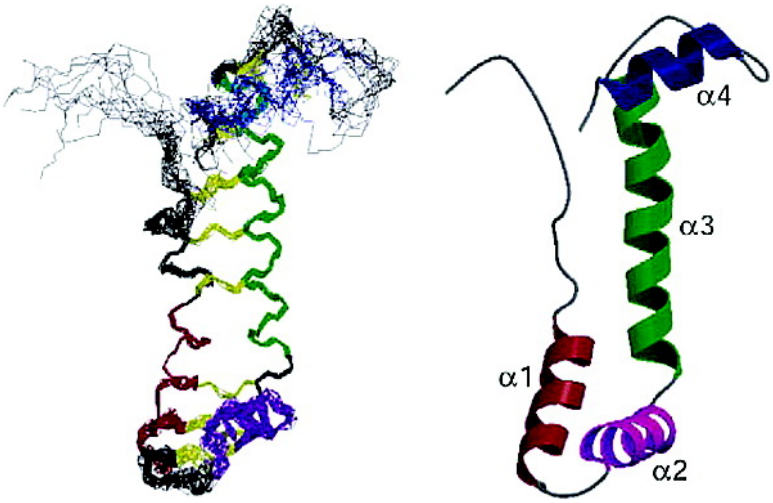

More About This Article

Additional resources and features associated with this article are available within the HTML version:

- Supporting Information
- Links to the 2 articles that cite this article, as of the time of this article download
- Access to high resolution figures
- Links to articles and content related to this article
- Copyright permission to reproduce figures and/or text from this article

View the Full Text HTML

J|A|C|S
ARTICLES
Published on Web 03/02/2005

Solution Structure of Vanabin2, a Vanadium(IV)-Binding Protein from the Vanadium-Rich Ascidian *Ascidia sydneiensis samea*

Toshiyuki Hamada,[†,‡] Miwako Asanuma,[†] Tatsuya Ueki,[§] Fumiaki Hayashi,[†] Naohiro Kobayashi,[†] Shigeyuki Yokoyama,[†] Hitoshi Michibata,[§] and Hiroshi Hirota*[,†,‡]

Contribution from RIKEN Genomic Sciences Center, 1-7-22 Suehiro-cho, Tsurumi-ku, Yokohama 230-0045, Japan, Division of Protein Folds Research, Graduate School of Integrated Science, Yokohama City University, 1-7-29 Suehiro-cho, Tsurumi-ku, Yokohama 230-0045, Japan, and Molecular Physiology Laboratory, Department of Biological Science, Graduate School of Science, Hiroshima University, Kagamiyama 1-3-1, Higashi-Hiroshima 739-8526, Japan

Received December 5, 2004; E-mail: hirota@gsc.riken.jp

Abstract: Ascidians belonging to the suborder Phlebobranchia are known to accumulate high levels of a transition metal, vanadium, in their blood cells, called vanadocytes, although the mechanism for this biological phenomenon remains unclear. Recently, we identified vanadium(IV)-binding proteins, designated as Vanabins, from vanadium-accumulating ascidians. Here, we report the first 3D structure of Vanabin2 from an ascidian, *Ascidia sydneiensis samea*, in an aqueous solution. The structure revealed a novel bow-shaped conformation, with four α-helices connected by nine disulfide bonds. There are no structural homologues reported so far. The ^{15}N heteronuclear single-quantum coherence (HSQC) perturbation experiments of Vanabin2 indicated that vanadyl cations, which are exclusively localized on the same face of the molecule, are coordinated by amine nitrogens derived from amino acid residues such as lysines, arginines, and histidines, as suggested by the electron paramagnetic resonance (EPR) results. The present NMR studies provide information that will contribute toward elucidating the mechanism of vanadium accumulation in ascidians.

Introduction

Since the beginning of the last century, it has been known that ascidians (tunicates or sea squirts) belonging to the suborder Phlebobranchia accumulate high levels of vanadium from seawater.[1−3] In a remarkable case, the concentration of cellular vanadium can approach 350 mM, corresponding to about 10 million times its concentration in seawater (35 nM).[4] This unusual phenomenon has been attracting the interdisciplinary attention of chemists, physiologists, and biologists. There is considerable interest in the possible role of vanadium in oxygen transport, as a putative third prosthetic group in respiratory pigments in addition to iron and copper, and the extraordinarily high levels of vanadium, which have never been reported in any other organism, except for a single species of polycheate worm.[5] Previously, we reported that vanadium ions in the +5 oxidation state [vanadium(V)] in seawater, are incorporated into the blood cells, called vanadocytes, and are stored in their vacuoles in the +3 oxidation state [vanadium(III)], which is rarely found in biological systems (Figure 1).[6,7] Several vanadium-binding proteins and vanadium-transporting proteins must be involved in the accumulation and reduction of vanadium in the vanadocytes.

Recently, we have identified a family of vanadium(IV)-binding proteins, designated as Vanabins, from a vanadium-rich ascidian, *Ascidia sydneiensis samea*. In this species, the Vanabin family consists of at least five closely related proteins. Among them, Vanabin1 and Vanabin2 were first extracted from the cytoplasmic fraction of vanadocytes as major vanadium-binding proteins.[8−10] Vanabin3 and Vanabin4 were then identified by an expressed sequence tag (EST) database analysis of vanadocytes,[11] and VanabinP was isolated from the ceolomic

[†] RIKEN Genomic Sciences Center.
[‡] Yokohama City University.
[§] Hiroshima University.

(1) Henze, M. *Hoppe-Seyler's Z. Physiol. Chem.* **1911**, *72*, 494−501.
(2) Michibata, H.; Terada, T.; Anada, N.; Yamakawa, K.; Numakunai, T. *Biol. Bull.* **1986**, *171*, 672−681.
(3) Michibata, H.; Yamaguchi, N.; Uyama, T.; Ueki, T. *Coord. Chem. Rev.* **2003**, *237*, 41−51.
(4) Michibata, H.; Iwata, Y.; Hirata, J. *J. Exp. Zool.* **1991**, *257*, 306−313.
(5) Ishii, T.; Nakai, I.; Numako, C.; Okoshi, K.; Ohtake, T. *Naturwissenschaften* **1993**, *80*, 268−270.
(6) Ueki, T.; Takemoto, K.; Fayard, B.; Salome, M.; Yamamoto, A.; Kihara, H.; Susini, J.; Scippa, S.; Uyama, T.; Michibata, H. *Zool. Sci.* **2002**, *19*, 27−35.
(7) (a) Hirata, J.; Michibata, H. *J. Exp. Zool.* **1991**, *257*, 160−165. (b) Kanamori, K.; Michibata, H. *J. Mar. Biol. Assoc. U.K.* **1994**, *74*, 279−286.
(8) Kanda, T.; Nose, Y.; Wuchiyama, J.; Uyama, T.; Moriyama, Y.; Michibata, H. *Zool. Sci.* **1997**, *14*, 37−42.
(9) Wuchiyama, J.; Nose, Y.; Uyama, T.; Michibata, H. *Zool. Sci.* **1997**, *14*, 409−414.
(10) Ueki, T.; Adachi, T.; Kawano, S.; Aoshima, M.; Yamaguchi, N.; Kanamori, K.; Michibata, H. *Biochim. Biophys. Acta* **2003**, *1626*, 43−50.
(11) Yamaguchi, N.; Kamino, K.; Ueki, T.; Michibata, H. *Mar. Biotechnol.* **2004**, *6*, 165−174.

10.1021/ja042687j CCC: $30.25

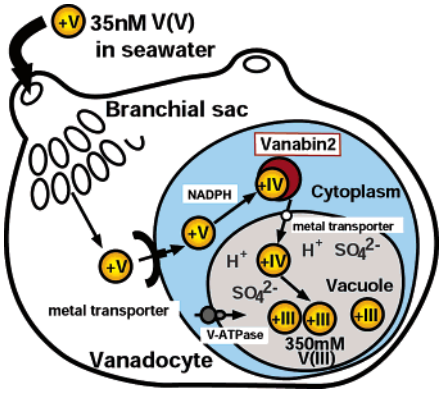

Figure 1. Schematic representation of vanadium accumulation and reduction by ascidians. The concentration of vanadium dissolved in seawater is only 35 nM in the +5 oxidation state. The vanadium(V) ions are assimilated by the vanadocytes of ascidians through metal transporters. In the vanadocytes, vanadium(V) ions are reduced to vanadium(IV) by NADPH, which is produced by the pentose phosphate pathway, with the assistance of a metal chelator. Vanabins are proposed to act as cytoplasmic carrier proteins for vanadium(IV) ions, like a copper chaperone for superoxide dismutase (SOD).[31] Vanabins may also chelate vanadium(V) and help in the reduction by NADPH. The vanadium(IV) ions are then transported into the vacuole by another metal transporter and reduced to vanadium(III) by an unknown mechanism. The vacuoles of vanadocytes are extremely acidic (pH 1.9 in *Ascidia gemmata*), and high concentrations of protons and sulfate ions coexist with vanadium(III) ions. The highest concentration of vanadium-(III) in the vacuole of *A. gemmata* approaches 350 mM.

fluid(H.M. et al., manuscript in preparation). A homology search with both the Vanabin1 and Vanabin2 sequences in BLASTP and public protein databases did not reveal any other proteins with striking similarities. On the other hand, we identified five new Vanabins (CiVanabin1 to CiVanabin5) by an EST database search of another vanadium-accumulating ascidian species, *Ciona intestinalis*, the whole genome of which has been sequenced, and have reported that these CiVanabins also bind vanadium(IV) ions.[12] We have also found similar genes from the related species *Ciona savignyi* (H.M. et al., manuscript in preparation). Vanabins, therefore, seem to be common among the vanadium-accumulating ascidians and to hold the key toward resolving the mechanism underlying the highly selective accumulation of vanadium ions.

Using recombinant Vanabin1 and Vanabin2, we revealed that they bind up to 10 and 20 vanadium ions in the +4 oxidation state [vanadium(IV)], with dissociation constants of 2.1×10^{-5} M and 2.3×10^{-5} M, respectively.[10] Most recently, an electron paramagnetic resonance (EPR) study revealed that Vanabin2 can bind up to ~23.9 vanadium ions/molecule, and most of the vanadium ions are in a mononuclear state and coordinated by amine nitrogens.[13] The EPR study also suggested that no allosteric effects are involved in the process of binding multiple vanadium ions. These data suggested that Vanabins are a new class of metal binding protein. Judging from their exclusive localization in the cytoplasm of vanadocytes,[8,9] Vanabin1 and Vanabin2 are considered to be vanadium metallochaperone proteins that transport vanadium ions from the cytoplasm to the vacuole, as illustrated in Figure 1.[3]

A better understanding of the functions of Vanabins and the mechanism of vanadium accumulation in ascidians requires high-quality 3D structures of the proteins in the presence and absence of vanadium ions. We report here the solution structure of Vanabin2, determined by multidimensional NMR experiments. The structure provides, to our knowledge, the first 3D picture of a protein with a novel protein fold that binds to multiple vanadium(IV) ions. There are no structural homologues reported so far. Moreover, the NMR titration experiments, showing the $^{1}H-^{15}N$ heteronuclear single-quantum coherence (^{15}N HSQC) spectra of Vanabin2 upon the gradual addition of VO^{2+} revealed the putative vanadium-binding sites on Vanabin2. The elucidation of this structure provides a key to solving a riddle that has attracted interdisciplinary interest for 90 years.

Results

MS and NMR Characterization of Vanabin2. Vanabin2 is composed of 91 amino acids, including 18 cysteines (Figure 2A). The electrospray ionization (ESI) mass spectrum of Vanabin2 showed a deconvoluted molecular mass at 10 467 Da, which is 18 mass units lower than the expected molecular mass of the protein in which all of the cysteine residues are reduced. Indeed, the complete reduction of Vanabin2 by dithio-1,4-threitol (DTT) caused the molecular weight (at 10 485 Da) to increase by 18 mass units, indicating that all 18 cysteine residues of Vanabin2 create intramolecular disulfide bonds. Therefore, the NMR study was carried out under nonreducing conditions.

^{15}N HSQC spectrum for the uniformly ^{15}N-labeled Vanabin2 showed cross-peaks that were well-dispersed (Figure 3A). Sequence-specific backbone and side-chain NMR signals were assigned by standard triple-resonance experiments with the $^{13}C,^{15}N$-labeled protein. Of the 95 amino acid residues, including four additional amino acids (I-S-E-F) derived from the junction region at the *N*-terminus, 82 residues were observed in the ^{15}N HSQC spectrum. However, no resonance signals from the residual eight amino acids, Ile1, Ser2, Thr33, Lys78, His79, His81, Lys82, and Asp84, were observed, presumably because of significant line broadening. The $^{13}C_{\beta}$ chemical shifts for the 18 cysteine residues are all largely downfield-shifted in the range of 36.4−48.5 ppm, indicating the formation of nine disulfide bonds.[14]

Disulfide Pairing Assignments. To determine the disulfide pairings, the structures were initially calculated with no disulfide constraints, and then the sulfur−sulfur and C_{β}/C_{β} distances for the possible pairings were compared. The results of this analysis are presented in Table 1. Assuming undistorted bond lengths and angles, the distance between the half-cystine C_{β} atoms across a disulfide bond ranges from 3.2 to 4.7 Å.[15] From the results shown in Table 1, the nine preferred disulfide pairings were assigned unambiguously, as Cys9−Cys63, Cys13−Cys59, Cys17−Cys56, Cys23−Cys49, Cys27−Cys44, Cys31−Cys40, Cys67−Cys94, Cys72−Cys89, and Cys76−Cys86.

The disulfide pairing of Cys9−Cys63 was also determined by the ESI-quadrupole time-of-flight (qTOF) MS analysis of the Lys-C digestion products of Vanabin2. In the MS analysis of the digestion products, a deconvoluted mass at 1492.7 Da (M + H) was assigned to peptide 63−65 linked to fragments 1−10, by the disulfide pairing between Cys9 and Cys63. The mass peaks of the other Lys-C digestion products are consistent

(12) Trivedi, S.; Ueki, T.; Yamaguchi, N.; Michibata, H. *Biochim. Biophys. Acta* **2003**, *1630*, 64−70.
(13) Fukui, K.; Ueki, T.; Ohya, H.; Michibata, H. *J. Am. Chem. Soc.* **2003**, *125*, 6352−6353.
(14) (a) Wishart, D. S.; Bigam, C. G.; Holm, A.; Hodges, R. S.; Sykes, B. D. *J. Biomol. NMR* **1995**, *5*, 67−81. (b) Sharma, D.; Rajarathnam, K. *J. Biomol. NMR* **2000**, *18*, 165−171.
(15) Manoleras, N.; Norton, R. S. *Biochemistry* **1994**, *33*, 11051−11061.

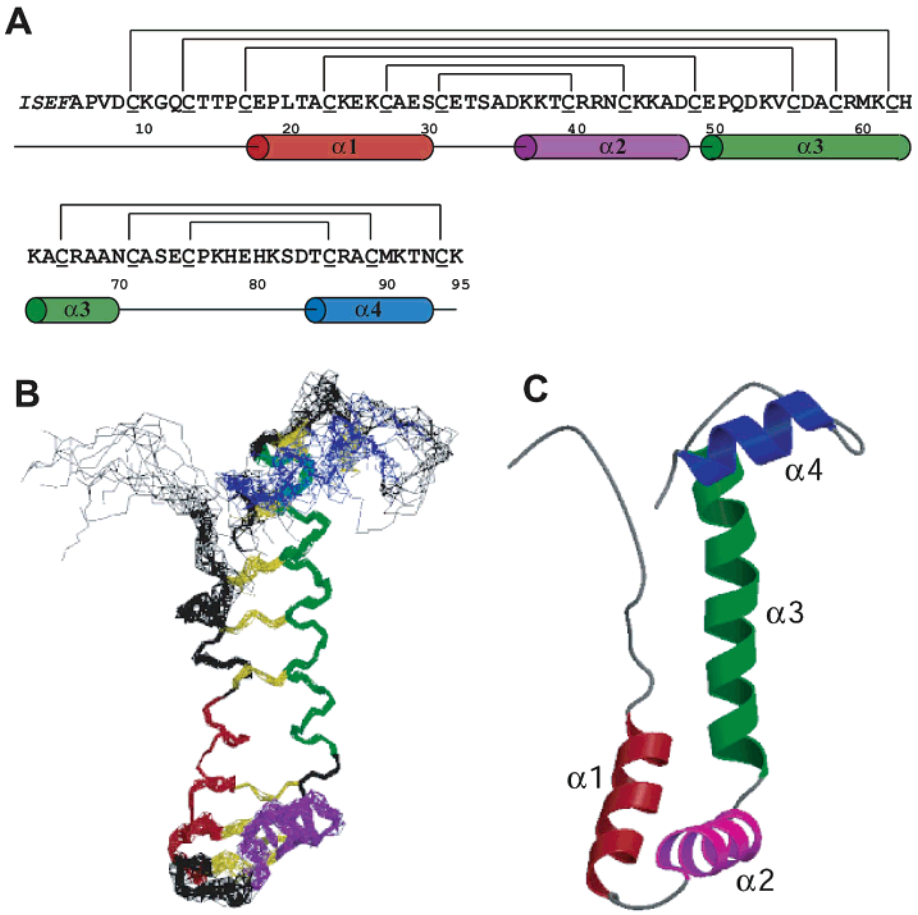

Figure 2. Structure of Vanabin2. (A) Amino acid sequence of Vanabin2.[10] The amino-terminal tag is italicized. The disulfide bond pairings, determined by the CYANA calculation, are indicated at the top of the sequence. The secondary structure elements of Vanabin2 are indicated at the bottom of the sequence and are colored correspondingly in all panels. (B) Final 10 structures superposed over the backbone heavy atoms of residues 18−70. The side chains of the half-cystine residues are shown as yellow lines. (C) Ribbon representation of a single structure, in the same orientation as in panel B.

Table 1. Calculated Distances for the Possible Half-Cystine Pairings of Vanabin2[a]

half-cystine pair	S/S distance[b] (Å)	C_β/C_β distance (Å)
9−63	4.45 ± 1.14	3.97 ± 0.62
13−59	5.01 ± 1.80	4.42 ± 0.36
17−56	3.47 ± 0.27	5.32 ± 0.69
23−49	3.66 ± 0.46	5.79 ± 0.33
27−44	3.40 ± 0.20	4.49 ± 0.23
31−40	3.56 ± 0.36	4.51 ± 0.38
67−94	4.56 ± 1.35	5.72 ± 1.05
72−89	3.93 ± 0.73	4.70 ± 0.56
76−86	3.55 ± 0.35	4.73 ± 0.35

[a] Structures were calculated by CYANA with no disulfide constraints. [b] All distances are mean ± SD.

with the above-determined disulfide pairings, although the confirmation of the other eight disulfide pairings by ESI-qTOF MS is in progress.

Structure Determination and Description. The final structure calculation was performed with the program CYANA[16] with the covalent bond information for the nine disulfide bonds. Figure 4 shows the summary of the sequential and medium-range ($1 < |i - j| < 5$) nuclear Overhauser effect (NOE) connectivities involving the NH, H_α, and H_β protons. The presence of helical structures encompassing residues 18−30, 37−48, 50−70, and 84−92 was indicated by the $d_{\alpha N}(i, i + 3)$, $d_{\alpha N}(i, i + 4)$, and $d_{\alpha\beta}(i, i + 3)$ connectivities, together with a strong intensities of the sequential NH−NH and H_β−NH cross-peaks.

Structures were calculated by use of 1141 upper-limit distance constraints inferred from NOEs, comprising 368 intraresidue, 312 sequential, 322 medium-range, and 139 long-range ($5 < |i - j|$) NOEs. In addition, 103 backbone dihedral angle constraints, based on the $^{13}C_\alpha$, $^{13}C_\beta$, ^{13}CO, $^{1}H_\alpha$, and ^{15}NH chemical shifts using the TALOS program,[17] and 14 χ_1 dihedral angle constraints, obtained by analyzing the HNHB and HN(CO)HB spectra,[18] were also employed for this calculation. Structures were refined by applying the calculation program CYANA. A summary of the statistics for these structures is given in Table 2. The 20 best structures (i.e., those with the lowest target functions < 0.1 Å^2) generated by the CYANA calculations have very small residual constraint violations, which indicate that the structures are consistent with the experimental constraints.

The overall conformation of Vanabin2 is shown in Figure 2B; the backbone heavy atoms of the 10 best structures (i.e., those with the lowest target functions) are superimposed between residues 18 and 70. The high convergence of the structures indicates that the structure is well defined throughout the

(16) Herrmann, T.; Güntert, P.; Wüthrich, K. *J. Mol. Biol.* **2002**, *319*, 209−227.
(17) Cornilescu, G.; Delaglio, F.; Bax, A. *J. Biomol. NMR* **1999**, *13*, 289−302.
(18) Bax, A.; Vuister, G. W.; Grzesiek, S.; Delaglio, F.; Wang, A. C.; Tschudin, R.; Zhu, G. *Methods Enzymol.* **1994**, *239*, 79−105.

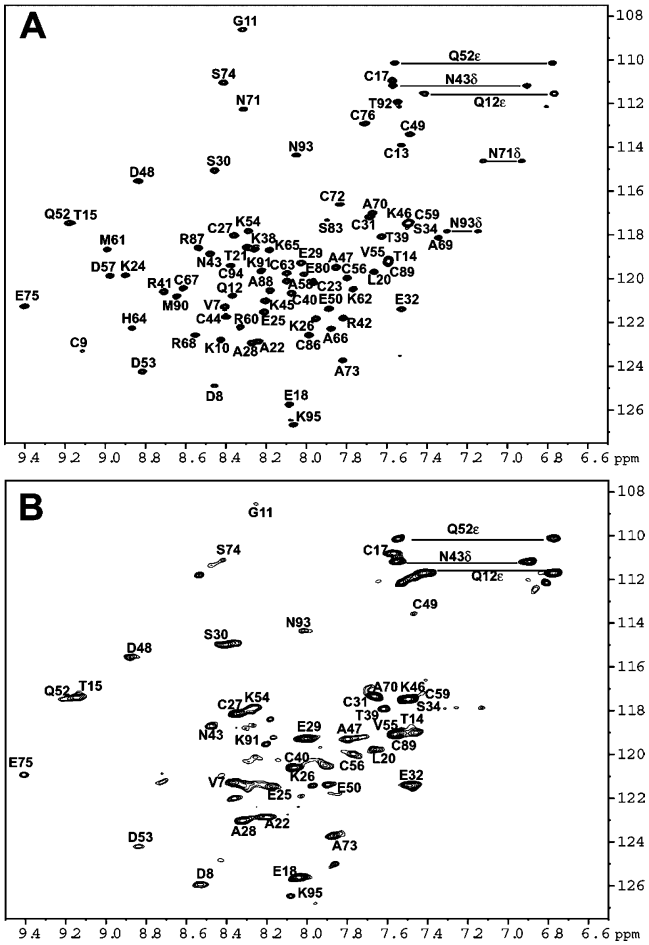

Figure 3. NMR spectra of free and vanadium(IV)-bound Vanabin2. Fully assigned ^{15}N HSQC spectra of 0.15 mM ^{15}N-labeled Vanabin2 in 20 mM potassium phosphate buffer, pH 6.9, in the absence (A) and presence (B) of 0.75 mM $VOSO_4$−IDA complex. The spectra were recorded at 30 °C on a 600 MHz spectrometer.

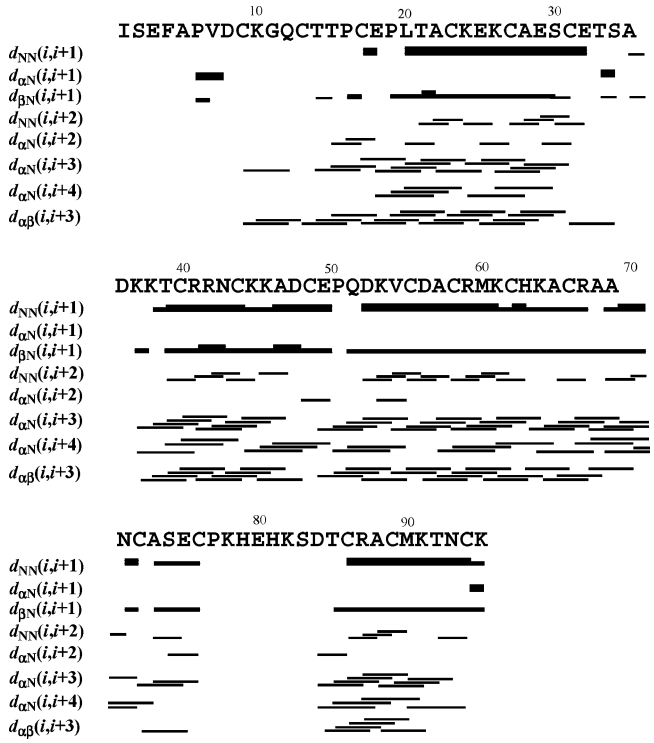

Figure 4. Summary of sequential and medium-range ($1 < |i - j| < 5$) NOEs involving NH, Hα, and Hβ protons in the ^{15}N- and ^{13}C-edited NOESY spectra of Vanabin2. The thickness of the bar represents the intensity of the cross-peaks. The symbols $d_{XY}(i, i + j)$ indicate the connectivity between the proton attached to atom X (backbone nitrogen N, α-carbon α, β-carbon β) and the proton attached to atom Y; the symbol i indicates the sequence from the jth amino acid.

sequence. The average atomic root-mean-square deviation (rmsd) value for the backbone atoms of the whole molecule is 1.1 Å, which is larger than that of each helix (0.2−0.3 Å), because there is no hydrophobic core in this molecule (Table 2). Ribbon representations of the backbone and disulfide bonds are shown in Figure 2C. The molecular architecture consists of an overall bow-shaped conformation with four α-helices (α1, 18−30; α2, 37−48; α3, 50−70; and α4, 84−92). The *N*-terminal segment (residues 10−18) seems to form a helix, but it could not defined because of insufficient NOE cross-peaks. There are nine disulfide bonds forming a ladder on the inner side of the molecule. Most of the χ_1 and some of the χ_2 torsion angles for the half-cystines are positioned well for stabilizing the shape of the whole molecule.

Interaction with Vanadium(IV) Ions. To analyze the interaction between vanadium(IV) ions and Vanabin2, an aqueous solution containing 1:1 equiv of $VOSO_4$ and iminodiacetic acid (IDA) was added to the Vanabin2 solution (pH 6.9) for NMR measurements. IDA was included to prevent the precipitation of vanadyl cations in the neutral pH range. Vanadium(IV) is a paramagnetic relaxation agent, which causes significant signal broadening and quenching of the resonance signals of residues located near the binding sites. The protein was titrated with various concentrations of vanadyl cations (VO^{2+}) (i.e., 0.2, 1.0, 5.0, 10, 20, and 40 mol equiv/protein). The ^{15}N HSQC spectrum of the ^{15}N-labeled Vanabin2 at a VO^{2+}/protein ratio of 5:1 (Figure 3B) shows that the resonances of residues 10, 12, 13, 21, 24, 38, 41, 42, 57, 58, 60−69, 71, 72, 76, 83−88, 90, and 94 had been quenched or disappeared, implying that these residues are located near the VO^{2+} interaction sites. The results from these ^{15}N HSQC perturbation experiments are summarized in the surface model of Vanabin2, where the quenched residues are highlighted (Figure 5A), indicating that the residues contacting the VO^{2+} ions are exclusively localized on one side of the molecule. Interestingly, the locations of the residues involved in the VO^{2+} interaction sites agree well with the blue-colored area in the electrostatic potential plot (Figure 5B), where the basic residues are gathered.

Discussion

Solution Structure and Vanadium−Protein Interaction. The phenomenon of vanadium accumulation by ascidians has been enigmatic for over 90 years. In the present study, we have obtained an important clue, which is the solution structure of the metal-free form of Vanabin2 from the vanadium-accumulating ascidian *A. sydneiensis samea*. The structure revealed a novel bow-shaped conformation, with four α-helices stabilized by the formation of nine disulfide bonds (Figure 3). A search for structurally similar proteins in the Protein Data Bank, using the distance matrix algorithm of the DALI program (version 2.0),[19] revealed no significantly similar proteins, indicating that Vanabin2 has a novel folding pattern.

(19) Holm, L.; Sander, C. *J. Mol. Biol.* **1993**, *233*, 123−138.

Table 2. Statistics for NMR Structure Calculations[a]

quantity	value[b]
residual CYANA target function[c] (Å^2)	0.14 ± 0.05
Residual NOE Distance Constraint	
no. > 0.1 Å	2 ± 2
maximum (Å)	0.12 ± 0.05
Residual Dihedral Angle Constraint	
no. > 2.5°	0 ± 0
maximum (deg)	1.33 ± 0.55
Residual Disulfide Bond Constraint	
no. > 0.1 Å	0 ± 0
maximum (Å)	0.02 ± 0.03
AMBER Energy (kcal /mol)	
total	−3093 ± 115
van der Waals	−258 ± 9
electrostatic	−3123 ± 126
RMSDs from Ideal Geometry	
bond lengths (Å)	0.01 ± 0.00
bond angles (deg)	1.87 ± 0.04
RMSDs from Average Structure (Å)	
backbone atoms for residues 5−95	1.12 ± 0.27
all heavy atoms for residues 5−95	1.65 ± 0.23
backbone atoms for residues 18−30	0.17 ± 0.06
all heavy atoms for residues 18−30	0.52 ± 0.05
backbone atoms for residues 37−48	0.30 ± 0.10
all heavy atoms for residues 37−48	0.96 ± 0.15
backbone atoms for residues 50−70	0.29 ± 0.13
all heavy atoms for residues 50−70	0.81 ± 0.11
backbone atoms for residues 84−92	0.26 ± 0.06
all heavy atoms for residues 84−92	0.73 ± 0.11

[a] Input consisted of 2686 NOE upper distance constraints and 117 dihedral angle constraints (103 of ϕ and ψ, and 14 of χ_1). [b] Average values + standard deviations for the 20 energy-minimized conformers with the lowest CYANA target function values are given. [c] Before energy minimization.

The ^{15}N HSQC perturbation experiments showed that the VO^{2+} ions are attached to a particular region of Vanabin2, where most of the basic residues, such as lysine and arginine, are localized. This observation corresponds well with a previous EPR study,[13] which proved that most of the EPR-active VO^{2+} ions are coordinated by amine nitrogens but not disulfide sulfurs. The VO^{2+}−amine nitrogen coordination must, therefore, be a key reaction of the vanadium−protein interaction process.

Biochemical Implications of Disulfide Bonds. Vanabin2 is a cytoplasmic protein,[8,9] and disulfide bonds are rarely found in such intracellular proteins. The reducing environment inside cells would result in the reduction of the cysteine residues in Vanabins, but all of the cysteine residues in Vanabin2 form disulfide bonds. Although rare, there are intracellular proteins with disulfide bonds, for example, thioredoxin and glutathione, which catalyze oxidation−reduction (redox) processes.[20] It is possible that Vanabins are enzymes involved in redox events in vanadocytes. The intracellular proteins of certain hyperthermophilic archaea are rich in disulfide bonds, implying that disulfide bonds stabilize many thermostable proteins.[21] Similarly, the disulfide bonds of Vanabin2 would significantly stabilize its native structure. In fact, the reduction of Vanabin2 with 200 mM DTT causes a dramatic loss of structure, as reflected in the ^{15}N HSQC spectrum of ^{15}N-labeled Vanabin2 (data not shown). Moreover, the binding of vanadium(IV) to Vanabin2 was strongly inhibited after the DTT treatment and was recovered after the DTT was removed (Figure 6). Thus, the presence of the disulfide bonds and the 3D structure appear to be crucial for the vanadium(IV)-binding activity of Vanabin2.

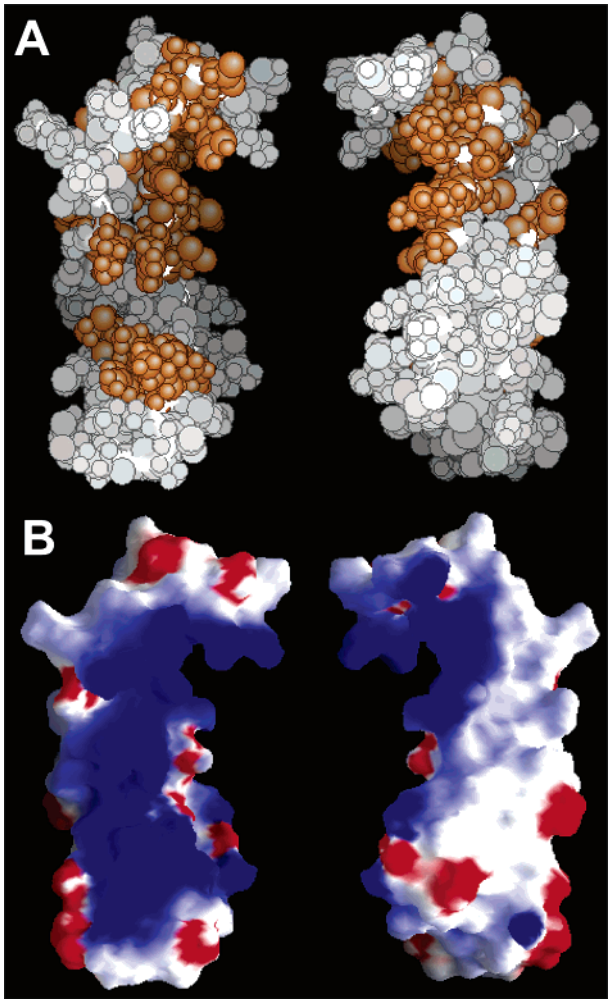

Figure 5. Surface of Vanabin2. (A) Vanadium binding sites are shown on the surface of the complexed Vanabin2; the color corresponds to the extent of quenching of the cross-peaks in the ^{15}N HSQC spectrum, induced by the addition of a 5-fold excess of vanadium(IV) ions, as shown in Figure 3B; residues with resonances that disappeared are colored orange. (B) Electrostatic surface potential of vanadium-free Vanabin2; positive charges are blue, and negative charges are red. Both figures are depicted with two faces looking in opposite directions.

Comparison with Other Vanadium-Binding Substances. To the best of our knowledge, there are four classes of substances that bind vanadium in the natural world: vanadium haloperoxidase (VHPO), vanadium nitrogenase (V-Nase), amavadine, and the Vanabins.[22] VHPOs are vanadate-dependent enzymes that catalyze the two-electron oxidation of a halide by hydrogen peroxide.[23] The mechanisms of vanadium ion binding and oxidative catalysis have been elucidated well by X-ray crystallographic studies and biochemical studies. VHPOs bind one or two vanadium(V) atoms per molecule, through several electrostatic interactions between vanadate and the

(20) (a) Prinz, W. A.; Aslund, F.; Holmgren, A.; Beckwith, J. *J. Biol. Chem.* **1997**, *272*, 15661−15667. (b) Choi, H. J.; Kim, S. J.; Mukhopadhyay, P.; Cho, S.; Woo, J. R.; Storz, G.; Ryu, S. E. *Cell* **2001**, *105*, 103−113. (c) Jakob, U.; Muse, W.; Eser, M.; Bardwell, J. C. A. *Cell* **1999,** *96*, 341−352.
(21) Mallick, P.; Boutz, D. R.; Eisenberg, D.; Yeates, T. O. *Proc. Natl. Acad. Sci. U.S.A.* **2002**, *99*, 9679−9684.
(22) Crans, D. C.; Smee, J. J.; Gaidamauskas, E.; Yang, L. *Chem. Rev.* **2004**, *104*, 849−902.
(23) Wever, R.; Hemrika, W. In *Handbook of Metalloproteins*; John Wiley & Sons: Ltd: Chichester, U.K., 2001; pp 1417−1428.

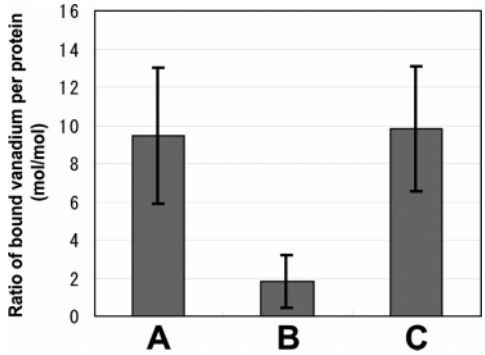

Figure 6. DTT-induced inhibition of the binding of vanadium(IV) ions to Vanabin2. Vanabin2 was loaded onto a gel equilibrated in binding buffer containing 50 μM vanadium(IV)−IDA. (A) Vanabin2 with no treatment; (B) Vanabin2 that had been incubated in the presence of 100 mM DTT for 45 min; (C) Vanabin2 after dialysis against binding buffer to remove the DTT. The vertical axis indicates the ratio of bound vanadium per protein (mol/mol) as the mean ± SD (n = 7−8).

positive and negative charges of Arg, Lys, His, and Asp in the binding pocket. V-Nases are vanadium-containing enzymes that catalyze the reduction of atmospheric N_2 to NH_3.[24] Although an apparently homogeneous mixture of proteins has hindered structural studies, mechanistic and modeling studies have proposed that V-Nases have Fe−S clusters coordinated with vanadium(V) as an active center.[25] On the other hand, amavadine is a natural bare V(IV) complex of (*S*,*S*)-2,2′-(hydroxyimido)-dipropionic acid extracted from some *Amanita* fungi, which acts as a peroxidase that catalyzes the oxidation of particular thiols to the corresponding disulfide compound.[26] Amavadine, with its unusual octacoordinated structure of the bare complex, might be involved in an electron-transfer process, although the biological role has not yet been clarified.[27] All three of these types of vanadium complexes have one or two vanadium atoms in their active centers that play enzymatic roles.

In contrast, most of the vanadium(IV) ions in Vanabins are in a mononuclear state and are coordinated by an amine nitrogen.[13] Furthermore, the Vanabins exhibit distinctly different vanadium binding properties; namely, Vanabin1 and Vanabin2 can bind to 20 and 10 vanadium(IV) ions, with moderate dissociation constants of 2.1×10^{-5} M and 2.3×10^{-5} M, respectively. These values are comparable to those of the nickel chaperone protein, UreE (1.0×10^{-5} M for Ni^{2+}), which assists in the insertion of Ni^{2+} into the active site of urease,[28] the copper-binding site of Menkes protein (4.5×10^{-5} M for Cu^{2+}),[29] and the periplasmic molybdate-binding protein ModA (3×10^{-6} M for molybdate and 5×10^{-6}M for tungstate).[30] In addition, Vanabins are localized in the cytoplasm of vanadocytes.[9] Since the cytoplasm of vanadocytes is not acidic, and free vanadium(IV) ions readily precipitate at neutral or higher pH values, we propose that the Vanabins function as a chelating compound to prevent the precipitation of vanadium(IV) ions. Considering their moderate dissociation constants, the Vanabins are presumed to work as cytoplasmic carrier proteins for vanadium(IV) ions, like the copper chaperone for superoxide dismutase (SOD).[31] Vanabins may also chelate vanadium(V) and help NADPH reduce vanadium(V) to vanadium(IV), which we will examine in our future research.

Although the unusual phenomenon whereby some ascidians accumulate vanadium to levels more than 10 million times higher than those in seawater has attracted researchers in various fields, the physiological roles of vanadium remain to be explained. Endean[32] and Smith[33] proposed that the cellulose of the tunic might be produced by vanadocytes. Carlisle suggested that vanadium-containing vanadocytes might reversibly trap oxygen under conditions of low oxygen tension.[34] The hypothesis has also been proposed that the vanadium in ascidians acts to protect them against fouling or as an antimicrobial agent.[35] However, most of the proposals do not seem to be supported by sufficient evidence. Therefore, we have obtained an important clue toward resolving the physiological roles of vanadium in ascidians. Attempts to inhibit the expression of the genes encoding Vanabins are expected to yield more information about the unusual accumulation of vanadium by this class of marine organisms.

Concluding Remarks

The present NMR study revealed the first detailed structure of one of the major vanadium-binding proteins, Vanabin2, and clarified the vanadium-binding sites on its structure. These results provide not only information on the structure and function of Vanabins but also important clues for solving the mechanism of vanadium accumulation in ascidians. The function of Vanabins *in vivo* remains to be identified, but our present results as well as previous studies strongly indicate that Vanabins transfer vanadium to another Vanabin or to a membrane receptor, analogous to the actions of the so-called metallochaperones (Figure 1).[31] The high levels of vanadium in ascidians still remain mysterious, both phylogenetically and functionally. Additional characterizations of the Vanabins are expected to assist in solving this mystery.

Experimental Section

Sample Preparation. The cloning, expression, and purification of Vanabin2 closely followed our previous methods.[10] To prepare ^{15}N- and ^{13}C,^{15}N-labeled Vanabin2, cells were grown in M9 minimal medium containing [^{15}N]NH_4Cl (1 g/L), with or without [^{13}C]glucose (2 g/L).

Mass Spectrometry. Mass spectra of Vanabin2 and its endoprotease Lys-C digestion products were obtained with a hybrid qTOF mass spectrometer (QSTAR, Applied Biosystems) equipped with an electrospray ion source. The samples were dissolved in acetonitrile/water (1:1 v/v) containing 0.1% formic acid.

NMR Spectroscopy. The NMR sample used for the structure determination was prepared by centrifugation with a Centricon YM3 filter (Millipore) and was analyzed as a protein solution (at approximately 1 mM) in 90% H_2O/10% D_2O containing 20 mM potassium phosphate buffer, pH 6.9. NMR spectra were acquired at 30 °C on

(24) Eady, R. R. *Coord. Chem. Rev.* **2003**, *237*, 23−30.
(25) Chen, J.; Christiansen, J.; Tittsworth, R. C.; Hales, B. J.; George, S. J.; Coucouvanis, D.; Cramer, S. P. *J. Am. Chem. Soc.* **1993**, *115*, 5509−5515.
(26) Bayer, E.; Kneifel, H. *Z. Naturforsch.* **1972**, *27B*, 207.
(27) Frausto da Silva, J. J. R. *Chem. Spec. Bioavailab.* **1989**, *1*, 139−150.
(28) Lee, M. Y.; Pankratz, H. S.; Wang, S.; Scott, R. A.; Finnegan, M. G.; Johnson, M. K.; Ippolito, J. A.; Christianson, D. W.; Hausinger, R. P. *Protein Sci.* **1993**, *2*, 1042−1052.
(29) Jensen, P. Y.; Bonander, N.; Moller, L. B.; Farver, O. *Biochim. Biophys. Acta* **1999**, *1434*, 103−113.
(30) Rech, S.; Wolin, C.; Gunsalus, R. P. *J. Biol. Chem.* **1996**, *271*, 2557−2562.
(31) Rae, T. D.; Schmidt, P. J.; Pufahl, R. A.; Culotta, T. C.; O'Halloran, T. V. *Science* **1999**, *284*, 805−808.
(32) (a) Endean, R. *Q. J. Microscop. Sci.* **1960**, *101*, 177−197. (b) Endean, R. *Austr. J. Mar. Freshwat. Res.* **1955**, *6*, 35−59. (c) Endean, R. *Austr. J. Mar. Freshwat. Res.* **1955**, *6*, 139−156.
(33) (a) Smith, M. *J. Biol. Bull.* **1970**, *138*, 345−378. (b) Smith, M. J. *Biol. Bull.* **1970**, *138*, 379−388.
(34) Carlisle, D. B. *Proc. R. Soc. London, B* **1968**, *171*, 31−42.
(35) Stoecker, D. *J. Exp. Zool.* **1983**, *227*, 319−322.

Varian Inova 600, Varian Inova 800, and Bruker Avance 600 spectrometers. Spectra were processed with the program NMRPipe,[36] and analyses of the processed data were performed with the programs NMRView[37] and Kujira (N.K. et al., unpublished method). Backbone and C_β proton resonances were assigned sequentially by use of two-dimensional (2D) ^{15}N HSQC, constant-time ^{13}C HSQC, and 3D HNCA, HN(CO)CA, HNCO, (HCA)CO(CA)NH, CBCA(CO)NH, and HNCACB spectra. Side-chain and C_α proton assignments were obtained from HBHA(CO)NH, C(CO)NH, HC(CO)NH, ^{15}N-edited total correlation spectroscopy (TOCSY), ^{15}N-edited NOESY, ^{13}C-edited NOESY, HCCH-COSY, and HCCH-TOCSY spectra. Distance constraints for structure calculations were obtained from ^{15}N-edited NOESY and ^{13}C-edited NOESY spectra. All NOESY spectra were measured with a 75-ms NOE mixing time. NOESY cross-peaks were picked and integrated by the Kujira program. The χ_1 torsion angles were determined from an analysis of the HNHB and HN(CO)HB spectra.[18]

Structure Calculations. A total of 2686 nuclear Overhauser effect spectroscopy (NOESY) cross-peaks were collected in the combined ^{15}N- and ^{13}C-edited NOESY spectra. The obtained peak lists (NOE and the chemical shift lists) were analyzed with the calculation program CYANA (http://www.guentert.com) for automated NOE assignment and structure calculation, which resulted in the clarification of 1141 NOE upper-limit distance constraints. The dihedral angle constraints ϕ and ψ were obtained by using the TALOS prediction[17] from the backbone ^{13}C chemical-shift values, such as $^{13}C_\alpha$, $^{13}C_\beta$, and ^{13}CO, and by analyzing the NOESY spectra. The constraints of the χ_1 torsion angles determined from the HNHB and HN(CO)HB spectra were established as three rotamers, ($-60° \pm 30°$, $180° \pm 30°$, and $60° \pm 30°$). By use of the distance constraints for the disulfide bonds obtained from the disulfide pairing analysis (Table 1), the final structure calculations with CYANA were started from 200 conformers with random torsion angle values. Simulated annealing with 15 000 time steps per conformer was done with the DYANA torsion angle dynamics algorithm[38] in CYANA.[16] To optimize energy force fields, the 20 conformers with the lowest final CYANA target function values were energy-minimized in a water shell by use of the AMBER force field[39] in OPALp.[40] Statistical data indicative of the quality and completeness of the structure determination are listed in Table 2. The structure was validated by PROCHECK-NMR.[41] Figures were generated with Molscript[42] and GRASP.[43] The atomic coordinates have been deposited in the Protein Data Bank, www.rcsb.org (PDB ID code 1VFI).

^{15}N HSQC Perturbation. The VO^{2+} titration was performed by recording a series of ^{15}N HSQC spectra with uniformly ^{15}N-labeled Vanabin2 (0.1 mM) in the presence of increasing amounts of a 1:1 mixture of vanadyl sulfate [vanadium(IV); $VOSO_4$] and iminodiacetic acid (IDA) ranging from 0.02 to 4.0 mM. IDA was included to prevent the precipitation of vanadium ions. The protein sample and the $VOSO_4$/IDA stock solution were prepared in the same buffer, containing 50 mM potassium phosphate, pH 6.8.

Metal Binding Assay. The Hummel-Dreyer method was used to determine the metal-binding ability of the recombinant Vanabins, as described previously.[10] A gel-filtration column (bed size 7 mm × 190 mm) filled with Bio-Gel P-6 DG resin (Bio-Rad Laboratories Inc.), which consists of polyacrylamide beads, was equilibrated with binding buffer (10 mM Tris-HCl and 100 mM NaCl, pH 7.4) containing the desired concentration of vanadium(IV)-IDA. Proteins were loaded onto the column and separated at a flow rate of 0.3 mL/min. Under these conditions, a protein peak appeared at around 5 min after loading. The metal concentration in each fraction was determined by atomic absorption spectrophotometry (AA-220Z, Varian Technologies Limited), and the protein concentration was determined with a Bio-Rad reagent (Bio-Rad Laboratories Inc.). The molar ratio of metal to protein was calculated for the fraction with the protein peak. Statistical significance was assessed by the Student's two-tailed *t*-test.

Acknowledgment. We thank Dr. Peter Güntert for setting up the software and writing several useful programs for NMR structure calculations. This work was supported in part by the National Project on Protein Structural and Functional Analyses, and in part by grants-in-aid (14340264 to H.M. and 14596005 to T.U.) from the Ministry of Education, Culture, Sports, Science, and Technology of Japan.

Supporting Information Available: Table of ^{15}N, ^{13}C, and ^{1}H resonance assignments of Vanabin2 at 300 K, pH 6.9, in buffer solution and ribbon representation of a single structure of Vanabin2 after the CYANA calculation with no disulfide bonds (PDF). This material is available free of charge via the Internet at http://pubs.acs.org.

JA042687J

(36) Delaglio, F.; Grzesiek, S.; Vuister, G. W.; Zhu, G.; Pfeifer, J.; Bax, A. *J. Biomol. NMR* **1995**, *6*, 277−293.
(37) Johnson, B.; Blevins, R. *J. Biomol. NMR* **1994**, *4*, 603−614.
(38) Güntert, P.; Mumenthaler, C.; Wüthrich, K. *J. Mol. Biol.* **1997**, *273*, 283−298.
(39) Cornell, W. D.; Cieplak, P.; Bayly, C. I.; Gould, I. R.; Merz, K. M.; Ferguson, D. M.; Spellmeyer, D. C.; Fox, T.; Caldwell, J. W.; Kollman, P. A. *J. Am. Chem. Soc.* **1995**, *117*, 5179−5197.
(40) Koradi, R.; Billeter, M.; Güntert, P. *Comput. Phys. Commun.* **2000**, *124*, 139−147.
(41) Laskowski, R. A.; Rullmann, J. A. C.; MacArthur, M. W.; Kaptein, R.; Thornton, J. M. *J. Biomol. NMR* **1996**, *8*, 477−486.
(42) Kraulis, P. J. *J. Appl. Crystallogr.* **1991**, *24*, 946−950.
(43) Occena, L. G.; Schmoldt, D. L. *Forest Prod. J.* **1996**, *46*, 40−42.